



Belgian Institute for Space Aeronomy  
(BIRA-IASB)




**SACS+**

**Extension of the  
“Support to Aviation Control Service”**

**Product Validation Document**


ESRIN/RFQ/3-12596/09/I-EC

*December 2010*

	<b>SACS+</b> Product Validation Document	<b>Ref.</b> SACSpus_PVD <b>Issue:</b> 1.0 <b>Date:</b> 10-12-2010 <b>Page:</b> 2 of 32
---	---	---

## Table of Contents

1	INTRODUCTION .....	3
1.1	Scope of this document.....	3
1.2	The SACS project.....	3
1.3	Acronyms and abbreviations .....	3
1.4	Applicable documents .....	5
2	INTERCOMPARISON OF SO <sub>2</sub> SATELLITE DATA PRODUCTS .....	6
2.1	UV-visible SO <sub>2</sub> columns observations.....	6
2.2	Comparison of UV-visible and infrared SO <sub>2</sub> observations.....	12
2.2.1	Comparisons between GOME-2 and IASI SO <sub>2</sub> data products .....	12
2.2.2	Comparisons between OMI and ASTER SO <sub>2</sub> data products.....	13
3	COMPARISON AGAINST GROUND-BASED MEASUREMENTS .....	16
4	INTERCOMPARISON OF AAI SATELLITE DATA PRODUCTS.....	19
4.1	Short Introduction.....	19
4.2	Intercomparison approach .....	19
4.3	First results – time series A .....	21
4.4	Improving the intercomparison – time series B.....	23
4.5	Scene dependencies .....	26
4.6	Discussion of results .....	30
5	REFERENCES.....	32

	<b>SACS+</b> Product Validation Document	<b>Ref.</b> SACSplus_PVD <b>Issue:</b> 1.0 <b>Date:</b> 10-12-2010 <b>Page:</b> 3 of 32
---	---	--

## 1 Introduction

### 1.1 Scope of this document

The present document provides elements of validation of the satellite nadir data products as part of the project SACS+ (extension of the “Support to Aviation Control Service”). A description of the algorithm theoretical basis related to these products can be found in [AD4].

### 1.2 The SACS project


The SACS (Support to Aviation Control Service) project is an ESA funded project aiming to deliver data in near-real time from measurements by space-based instruments regarding sulphur dioxide (SO<sub>2</sub>) and aerosol emissions possibly related to volcanic eruptions. This is achieved using polar-orbiting satellite instruments, measuring in the UV-visible (SCIAMACHY, OMI and GOME-2) and the infrared (IASI). SACS primary objective is to support the Key Users of the service (the Volcanic Ash Advisory Centres -VAACs) by sending an alert by email in case of exceptional concentrations of SO<sub>2</sub> detected. The User is then redirected to a single user-friendly web portal (<http://sacs.aeronomie.be>) centralizing maps, data (including archive) and useful information.

In this document, the consistency of the SO<sub>2</sub> products is explored by performing various intercomparisons of satellite-based SO<sub>2</sub> column data products, as well as comparisons with SO<sub>2</sub> observations from selected ground-based instruments.


It should be noted here that validation of satellite-based SO<sub>2</sub> data products is limited, because of the difficulties involved in comparisons between ground-based and satellite-based data, as well as difficulties in the comparison of the data from different satellites. These difficulties are, for example, related to measuring different air masses at different moment of the day.

### 1.3 Acronyms and abbreviations

AAI	Absorbing Aerosol Index
AMF	Air Mass Factor
ASCII	American Standard Code for Information Interchange
ASTER	Advanced Spaceborne Thermal Emission and Reflection Radiometer
ATBD	Algorithm Theoretical Basis Document
BIRA-IASB	Belgian Institute for Space Aeronomy
BTD	Brightness Temperature Difference
CCD	Charge-Couple Device
CEOS	Committee on Earth Observation Satellites
CMA	Center of Mass Altitude

	<b>SACS+</b> Product Validation Document	<b>Ref.</b> SACSpplus_PVD <b>Issue:</b> 1.0 <b>Date:</b> 10-12-2010 <b>Page:</b> 4 of 32
--	---	---


DOAS	Differential Optical Absorption Spectrometry
DLR	German Aerospace Center
DU	Dobson Unit
DUE	Data User Element
ECMWF	European Centre for Medium-Range Weather Forecasts
ENVISAT	ENVironmental SATellite
EOS	Earth Observation System
EPP	Equator Passing Point
ESA	European Space Agency
ESRIN	European Space Agency Research Institute
EUMETSAT	EUropean organization for the exploitation of METeorological SATellites
FRESCO	Fast Retrieval Scheme for Cloud Observables
GOME-2	Global Ozone Monitoring Instrument (aboard MetOp)
HDF	Hierarchical Data Format
IASI	Infrared Atmospheric Sounding Interferometer (aboard MetOp)
IAVW	International Airways Volcano Watch
ICAO	International Civil Aviation Organization
IR	Infrared
KMI-IRM	Royal Meteorological Institute of Belgium
KNMI	Royal Netherlands Meteorological Institute
LF	Linear Fit
LIDORT	Linearized Discrete Ordinate RTM
LUT	Look-Up-Table
MetOp-A	Meteorological Operational satellite-A
N/A	Not Applicable
NASA	National Aeronautics and Space Administration
NRT	NRT
O3MSAF	Ozone Monitoring Satellite Application Facility
OMI	Ozone Monitoring Instrument
PBL	Planetary Boundary Layer
PVD	Product Validation Document
RCP	Radiative Cloud Pressure
RTM	Radiative Transfer Model
SACS	Support to Aviation Control Service
SAVAA	Support to Aviation for Volcanic Ash Avoidance
SCD	Slant Column Density
SCIAMACHY	SCanning Imaging Absorption spectroMeter for Atmospheric CartographY (aboard ENVISAT)
SPSD	Service Portfolio Specification Document
STL	STratospheric Low
SO2	Sulfur Dioxide
SZA	Solar Zenith Angle
TBD	To Be Defined / Described
TOA	Top Of the Atmosphere

	<b>SACS+</b> Product Validation Document	<b>Ref.</b> SACSpus_PVD <b>Issue:</b> 1.0 <b>Date:</b> 10-12-2010 <b>Page:</b> 5 of 32
--	---	---

TOMS	Total Ozone Mapping Spectrometer
TRL	TRoposphere Low
TRM	TRoposphere Middle
UK	United Kingdom
ULB	Université Libre de Bruxelles
US	United States
UTC	Universal Time Coordinated
UV-VIS	Ultraviolet-Visible
VAAC	Volcanic Ash Advisory Centre
VCD	Vertical Column Density
VZA	Viewing Zenith Angle

#### 1.4 Applicable documents

- [AD1] ESA/ESRIN Statement of Work, ref. CEOS-INPR-EOPG-SW-09-0001, issued February 2009, of ESRIN/RFQ/3-12596/09/I-EC, Issue 1 rev 1.
- [AD2] SACS+: Extension of the “Support to Aviation Control Service” in Support of the CEOS Atmospheric Composition Constellation, I: Technical Proposal, issued June 2009.
- [AD3] SACS+: Extension of the “Support to Aviation Control Service” in Support of the CEOS Atmospheric Composition Constellation, I: Management Proposal, issued June 2009.
- [AD4] SACS+: Extension of the “Support to Aviation Control Service”, Algorithm Theoretical Basis Document, issued November 2010.

	<b>SACS+</b> Product Validation Document	<b>Ref.</b> SACSplus_PVD <b>Issue:</b> 1.0 <b>Date:</b> 10-12-2010 <b>Page:</b> 6 of 32
---	---	--

## 2 Intercomparison of SO<sub>2</sub> satellite data products

### 2.1 UV-visible SO<sub>2</sub> columns observations

The difference in time of the GOME-2 and SCIAMACHY measurements is about 40 minutes and the two are in approximately the same orbit. During that time any SO<sub>2</sub> will have moved a little and the cloud situation will be somewhat different, but a direct comparison of respective measurements is still possible. OMI measures 2-4 hours later (depending on the location on Earth) and a direct comparison with SCIAMACHY or GOME-2 therefore has limited value.

#### Comparsion exercise for SO<sub>2</sub> in the stratosphere

On 7 August 2008 the Kasatochi volcano on one of the Aleutian Islands (52.17N, 175.51W; summit 314 m) erupted, a volcano that had not been active for more than 200 years. The eruption took place in at least three phases between about 20h UTC on 7 August and 04h30 UTC on 8 August and emitted large amounts of SO<sub>2</sub> into the atmosphere, reaching an altitude of about 12 km. Figure 1 shows the SO<sub>2</sub> distribution as observed by GOME-2, SCIAMACHY and OMI on 8 August. For comparison, also the cloud cover fraction taken from the GOME-2 level-2 data product is shown.

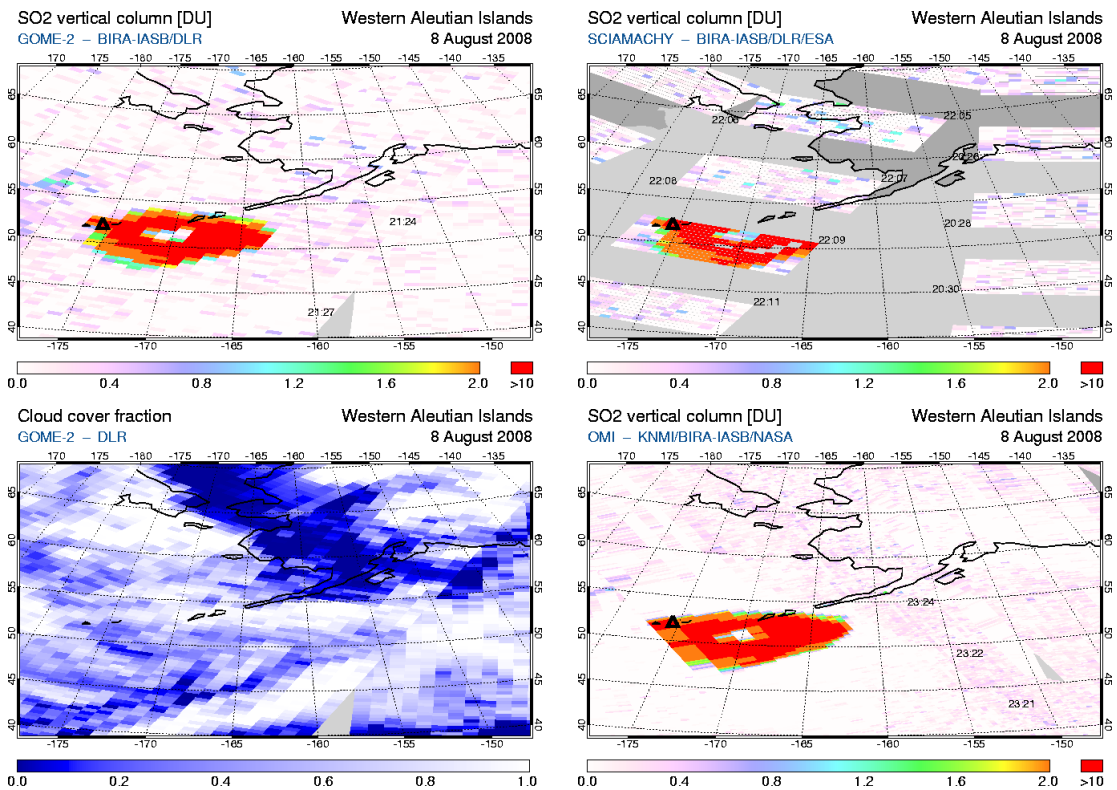


Figure 1 : Total column  $\text{SO}_2$  distribution on 8 August 2008 as measured by GOME-2 (top-left), SCIAMACHY (top-right) and OMI (bottom-right), as well as the cloud cover fraction from GOME-2 (bottom-left). The  $\text{SO}_2$  was emitted during the eruption of the Kasatochi volcano. The numbers in the  $\text{SO}_2$  graphs show the measurement times in UTC – for GOME-2 at the begin and end of each PDU, for SCIAMACHY at begin and end of each nadir state, and for OMI at the centre of the orbit, one every 50 scans.

The  $\text{SO}_2$  patch occurs in nicely overlapping GOME-2 and SCIAMACHY orbits and so a direct comparison on a pixel-to-pixel basis is possible. To that end an along-track and along-scan line through the GOME-2 orbit are defined and the corresponding track and scan of SCIAMACHY are determined – see Figure 2. The match is not perfect, but near enough for a comparison.

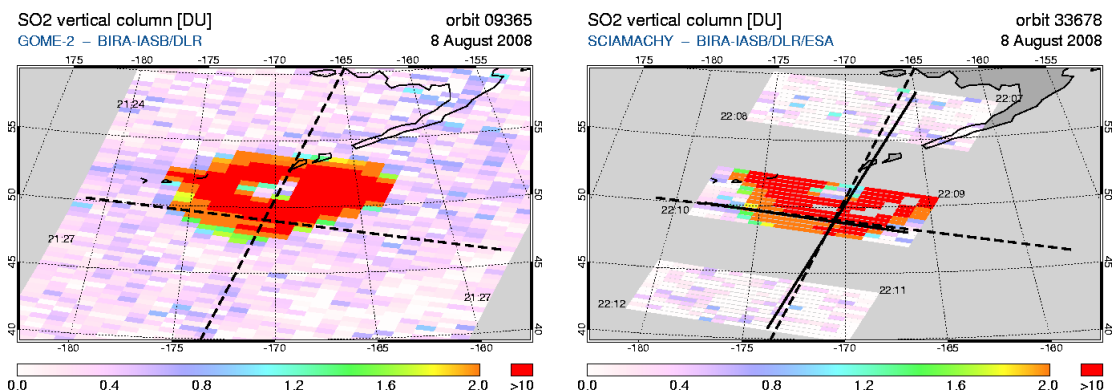



Figure 2: Along-track and along-scan lines in the GOME-2 (dashed) and SCIAMACHY (solid) orbit used for a direct pixel-to-pixel comparison of data on 8 August 2008.

	<b>SACS+</b> Product Validation Document	<b>Ref.</b> SACsplus_PVD <b>Issue:</b> 1.0 <b>Date:</b> 10-12-2010 <b>Page:</b> 8 of 32
---	---	--

Along-track and along-scan matches can only be used in cases where GOME-2 and SCIAMACHY orbits fully overlap, and the higher the latitude, the larger the angle between the comparison lines. And even then the (almost) match works only for about three SCIAMACHY nadir states. The focus lies here mainly on the central of these three nadir states, with the peak of the SO<sub>2</sub> cloud.

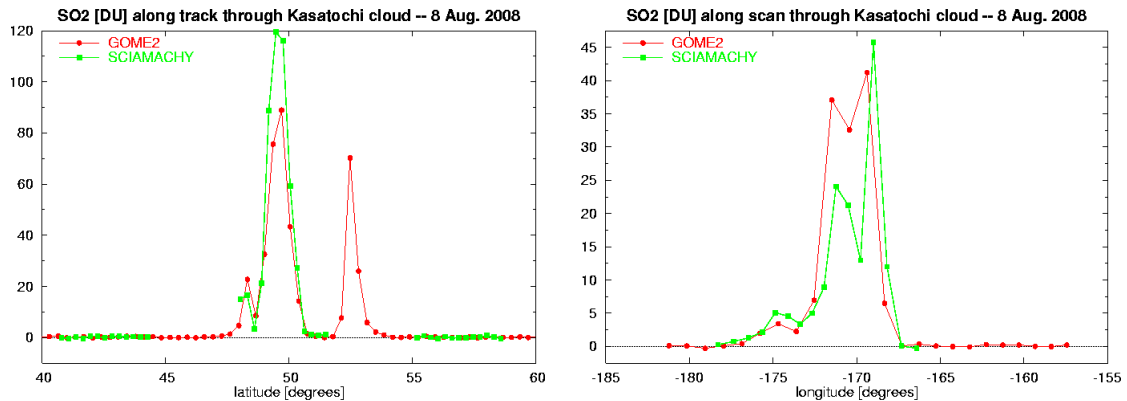


Figure 3: Comparison of the total SO<sub>2</sub> column from GOME-2 and SCIAMACHY for the along-track lines (left) and along-scan lines (right) drawn in Figure 2.

The results of the pixel-to-pixel comparison along the lines in Figure 2 are shown in Figure 3. Since the SO<sub>2</sub> cloud is certainly in the lower stratosphere – most likely at around 12 km altitude – the comparison is done using the data set based on a stratospheric SO<sub>2</sub> plume.

The match between the location and magnitude of the SO<sub>2</sub> peak along and across the track is very good, especially if one takes into account that there must have been quite some dynamical motion in the SO<sub>2</sub> cloud during the 40 minutes time difference. The maximum SO<sub>2</sub> values from SCIAMACHY are about 25 % higher compared to the GOME-2 columns. The resolution in the across-track direction of SCIAMACHY is higher than GOME-2's resolution, which means that the match along the scan (right in Figure 3) will always be a little less accurate than a match along a track.

Three days later, on 11 August, the SO<sub>2</sub> cloud lies off the coast of Alaska and another almost-match can be found, as Figure 4 shows. Again the along-track match deviates about 1 SCIAMACHY ground pixel to the end of the depicted range, but the comparison can still be made.



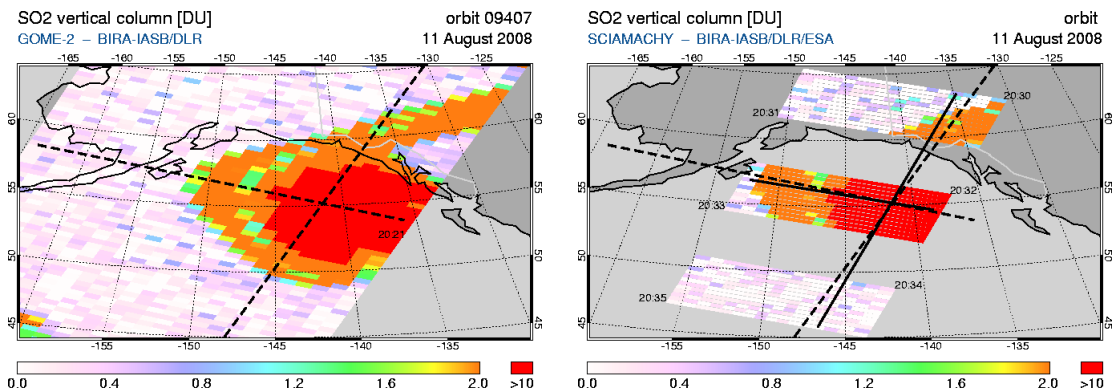


Figure 4: Along-track and along-scan lines in the GOME-2 (dashed) and SCIAMACHY (solid) orbit used for a direct pixel-to-pixel comparison of data on 11 August 2008.

The results of the comparisons along the lines in Figure 4 are shown in Figure 5. The comparison of the SO<sub>2</sub> total column shows that both instruments capture the structure of the SO<sub>2</sub> cloud very well, the locations of the peak SO<sub>2</sub> values and the dimensions of the SO<sub>2</sub> cloud match nicely for both instruments. Differences can be found in the total SO<sub>2</sub> columns, SCIAMACHY gives total columns that are of the order of 20 DU higher. A similar difference is seen in the comparison in Figure 3, at least in the along-track comparison, though less clear because the SO<sub>2</sub> cloud is smaller in size. Note that the difference in SO<sub>2</sub> columns is not related to cloud issues.

One important difference between the SO<sub>2</sub> slant column retrieval from SCIAMACHY and GOME-2 is the use of different cross-sections at different temperatures. GOME-2 uses reconvolved SCIA FM cross-sections at a temperature representative for the specific height, in this case a stratospheric temperature for the 15 km retrieval, while for the SCIAMACHY retrieval a cross-section at a tropospheric temperature is used. This can result in up to 20% higher slant columns and could therefore explain part of the difference in SO<sub>2</sub> column. Another issue that could induce differences in the retrieved slant columns is the choice of the reference spectra, for the GOME-2 retrieval a daily solar spectrum is used, whereas the SCIAMACHY retrieval uses an earthshine spectrum as reference (selected from an equatorial region without SO<sub>2</sub> sources).

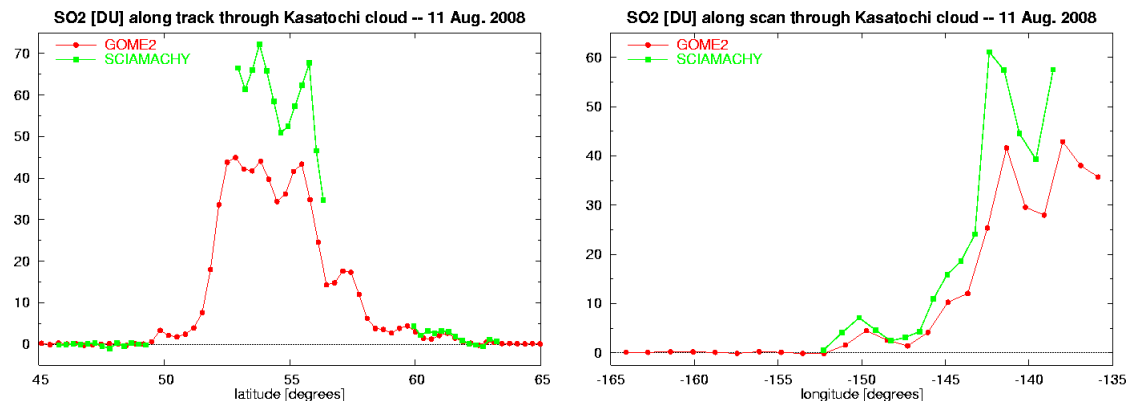



Figure 5: Comparison of the total SO<sub>2</sub> column from GOME-2 and SCIAMACHY for the along-track lines (left) and along-scan lines (right) drawn in Figure 4.

	<b>SACS+</b> Product Validation Document	<b>Ref.</b> SACSplus_PVD <b>Issue:</b> 1.0 <b>Date:</b> 10-12-2010 <b>Page:</b> 10 of 32
--	---	---

## Comparison exercise for SO<sub>2</sub> in the mid-troposphere

The Kilauea volcano on Hawaii (19.42N, 155.29W; summit 1222 m) started a new period of activity in March 2008, with a large number of low-level eruptions. The SO<sub>2</sub> emitted by the volcano seems to remain mostly in the neighbourhood of the volcano and remains visible for a day or two. This implies that the SO<sub>2</sub> is emitted at low altitudes, in the troposphere, where the lifetime of SO<sub>2</sub> is a few days. The total amounts of SO<sub>2</sub> emitted are not very large, with concentrations between 5 and 15 DU. The series of Kilauea eruptions can therefore be used for comparing low-level SO<sub>2</sub> concentrations in the middle troposphere. Since the SO<sub>2</sub> cloud of the volcano is limited in size, the situation can also be used to compare background SO<sub>2</sub> concentrations.

Consider as an example the SO<sub>2</sub> plume west of Hawaii on 17 May 2008. Figure 6 shows the GOME-2 and SCIAMACHY orbits that passed over the plume that day. These orbits overlap completely and it is easy to find matching along-track and along-scan lines suitable for a comparison, because at this latitude the tracks of the instruments run nicely parallel. Due to the ground pixel widths of 60 km for SCIAMACHY and 80 km for GOME-2, a match is found every three GOME-2 tracks. Let us therefore look at a set of four tracks and three scans for the comparison.

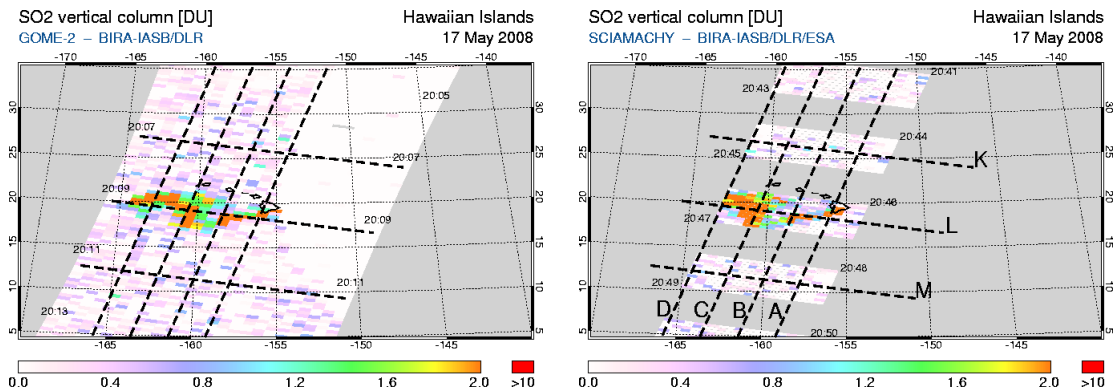


Figure 6: SO<sub>2</sub> distribution for GOME-2 orbit 8185 (left) and SCIAMACHY orbit 32490 (right), which passed over Hawaii on 17 May 2008. The dashed lines are used for along-track and along-scan comparisons, labelled with the letters in the right plot.

Figure 7 shows the comparisons of the SO<sub>2</sub> total columns along the four tracks A – D and the three scans K – M. The correspondence between the SO<sub>2</sub> columns from GOME-2 and SCIAMACHY for these tracks and scans is very good.

The peak values of the SO<sub>2</sub> total columns correspond very well. This shows that the differences in SO<sub>2</sub> peak values found in the previous comparison exercise (Kasatochi eruption), when looking at very high SO<sub>2</sub> concentrations in the lower stratosphere, are limited mainly to that situation. The fact that the SO<sub>2</sub> cross-sections are used at different temperatures for the two instruments plays less of a role for tropospheric SO<sub>2</sub> as the temperature difference is smaller.

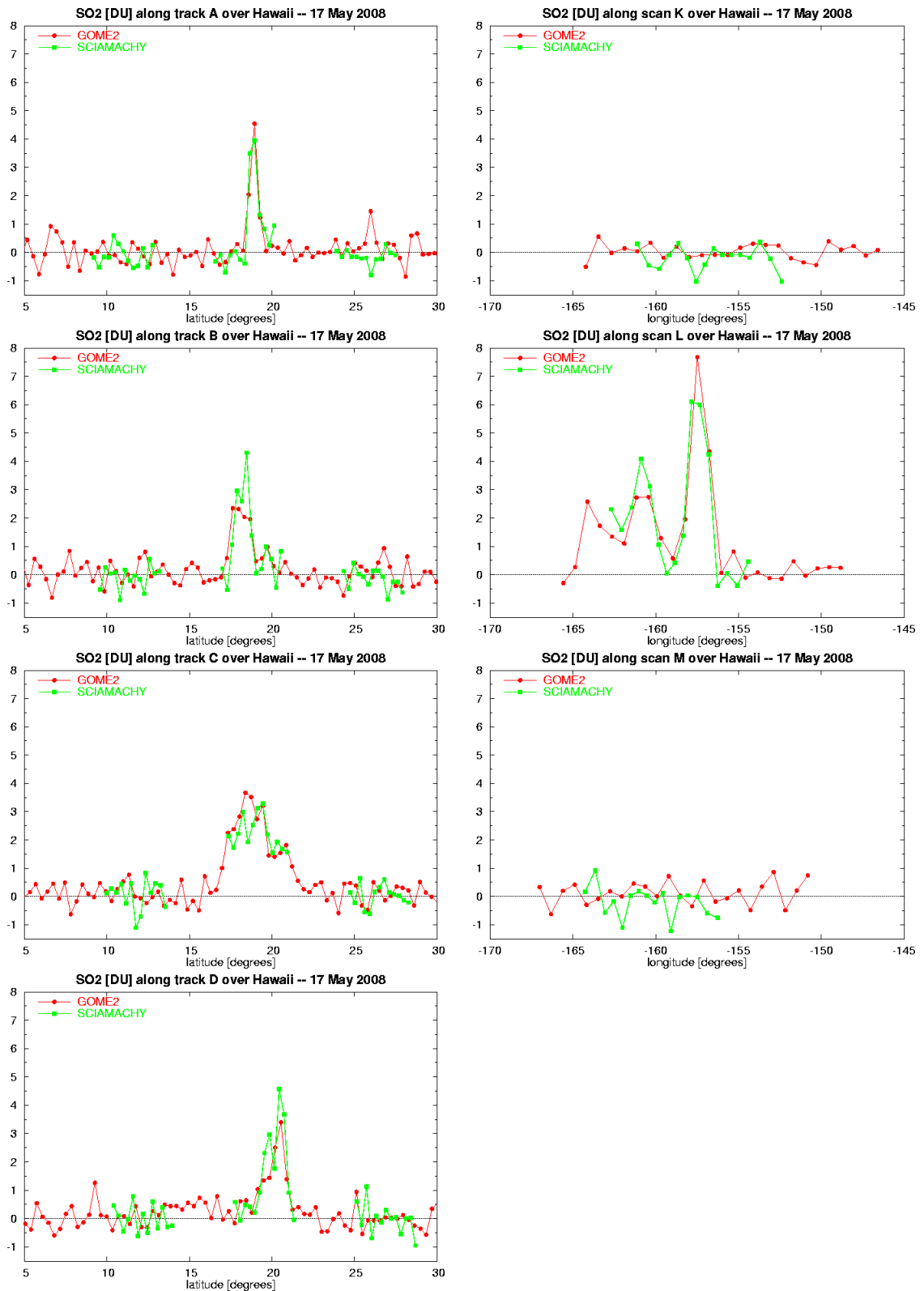



Figure 7: Comparison of the total SO<sub>2</sub> column from GOME-2 and SCIAMACHY for the along-track lines A – D and for the along-scan lines K – L drawn in Figure 6.

	<b>SACS+</b> Product Validation Document	<b>Ref.</b> SACSplus_PVD <b>Issue:</b> 1.0 <b>Date:</b> 10-12-2010 <b>Page:</b> 12 of 32
---	---	---

## 2.2 Comparison of UV-visible and infrared SO<sub>2</sub> observations

### 2.2.1 Comparisons between GOME-2 and IASI SO<sub>2</sub> data products

Whereas both satellite UV and IR sensors are sensitive to SO<sub>2</sub> from volcanoes, they are however characterized by different vertical measurement sensitivity. Therefore it makes any comparison between UV and IR SO<sub>2</sub> products rather complicated, unless additional information on the altitude of the plume is provided. In this section, we make no attempt to compare quantitatively the SO<sub>2</sub> products from UV and IR sensors. Conversely, we compare by-eye the patterns of elevated SO<sub>2</sub> as observed by GOME-2 and IASI, instruments for which the ability to track volcanic clouds have been extensively demonstrated. Here we take advantage of the fact that both GOME-2 and IASI (daytime) observations are quasi collocated, as both instruments are operating on the same platform (MetOp-A). Figure 8 shows examples of volcanic SO<sub>2</sub> plumes observed by GOME-2 (SO<sub>2</sub> vertical columns) and IASI (SO<sub>2</sub> brightness temperature index in the v3 band) after recent eruptions (namely Redoubt in Alaska, Eyjafjallajokull in Iceland and Pacaya in Guatemala). Besides the different spatial resolution of both instruments, a very good correlation between GOME-2 and IASI observations of the plumes is visible, for all three days of measurements in Figure 8. There are some differences for filamentary structures of the plumes (e.g., Eyjafjallajokull plume), but they can largely be explained by the different vertical measurement sensitivity of GOME-2 and IASI for SO<sub>2</sub> air mass transport to lower altitudes.

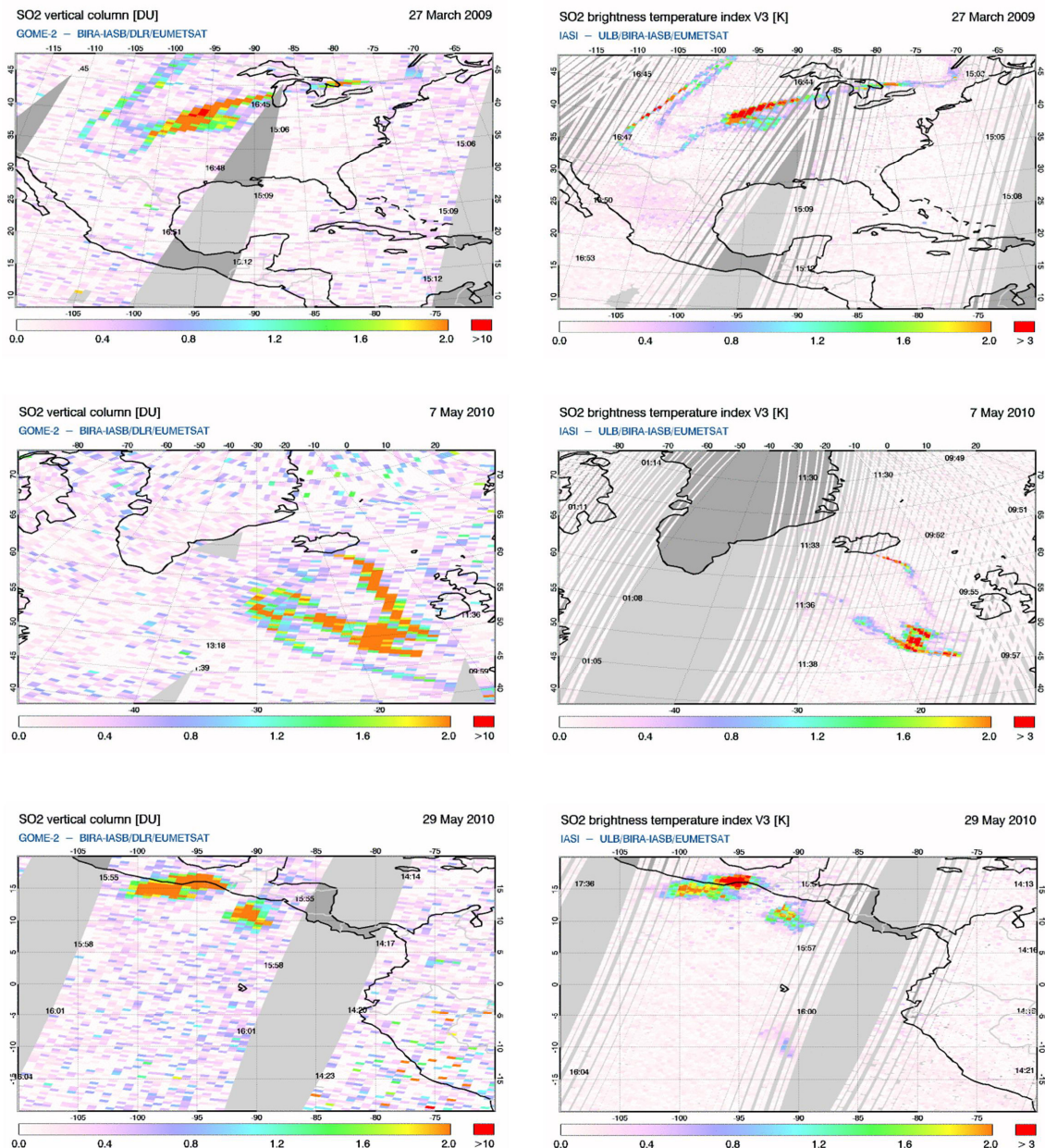



Figure 8: Qualitative comparison the total SO<sub>2</sub> column from GOME-2 and the SO<sub>2</sub> index from IASI (daytime observations) for three days (27/03/2009, 07/05/2010 and 29/05/2010) all related to recent eruptions (Redoubt in Alaska, Eyjafjallajokull in Iceland, Pacaya in Guatemala).

## 2.2.2 Comparisons between OMI and ASTER SO<sub>2</sub> data products

Here we present comparisons between the OMI SO<sub>2</sub> product and ASTER data (see details in Pinardi et al., 2010). The Advanced Spaceborne Thermal Emission and Reflection Radiometer (ASTER; Pieri and Abrams, 2004) is an imaging instrument operating onboard EOS/Terra that has the capability to provide SO<sub>2</sub> vertical columns (data obtained from R. Campion, personal communication) with a very high spatial

	<b>SACS+</b> Product Validation Document	<b>Ref.</b> SACSplus_PVD <b>Issue:</b> 1.0 <b>Date:</b> 10-12-2010 <b>Page:</b> 14 of 32
---	---	---

resolution of 90x90 m<sup>2</sup> and enables to observed fine spatial structures of volcanic plumes. One way to deal with the different spatial resolution of OMI and ASTER (as illustrated in Figure 9 for the eruption of Etna: 03/08/2006) as well as differences in the SO<sub>2</sub> retrieval is to compare estimates of SO<sub>2</sub> fluxes as emitted during a given volcanic eruption.

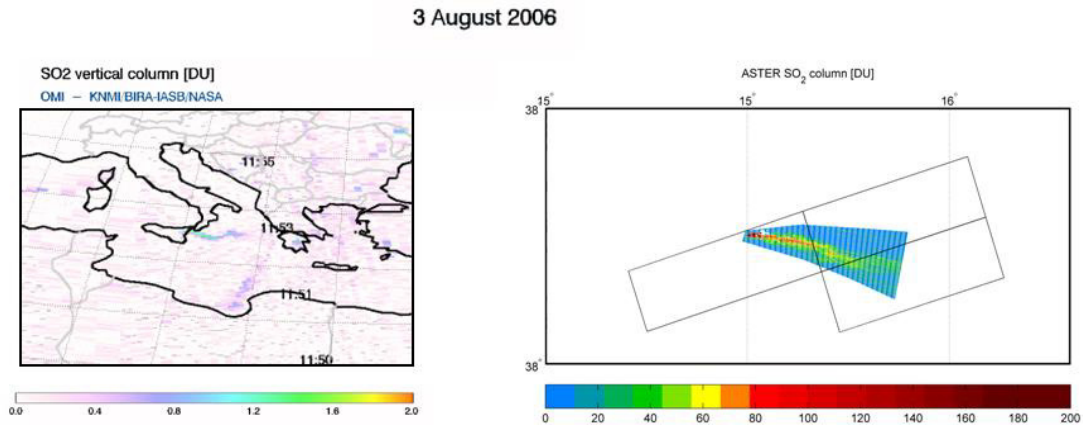


Figure 9: SO<sub>2</sub> vertical columns in the vicinity of Etna on the 3<sup>rd</sup> of August 2006 as observed by OMI and ASTER (the edges of the three closest OMI pixels are also depicted in black).

A flux calculation routine initially developed for the ASTER data (Campion et al., 2010) has also been applied to OMI for a series of recent eruptions. It uses the SO<sub>2</sub> column amounts, an estimation of the altitude of the volcanic plume and ECMWF wind fields. As shown in Figure 10, the results are calculated along parallel transects of the plumes at various distance from the volcano.

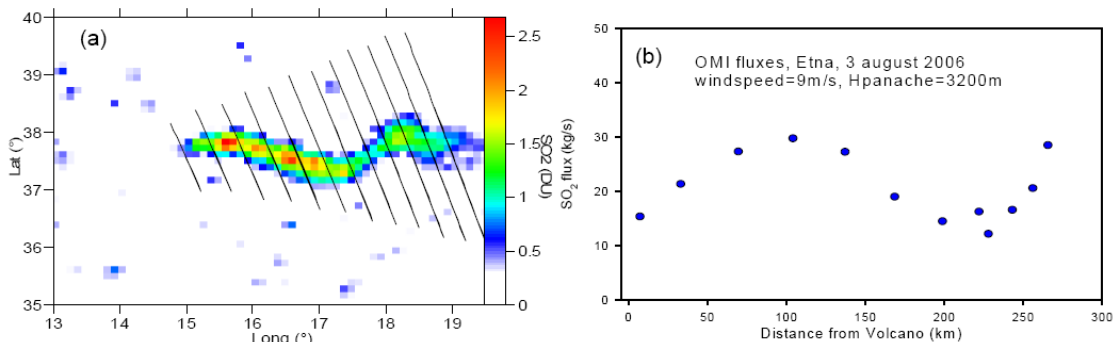


Figure 10: SO<sub>2</sub> vertical columns observed by OMI after the eruption of Etna (3<sup>rd</sup> of August 2006) with the different transects (left) used to calculate the SO<sub>2</sub> as a function of the distance from the volcano (right).

Figure 11 shows the comparison of the fluxes averaged for the OMI and ASTER data for several recent volcanic plumes from Etna, Nyriagongo, Nyamuragira and Anatahan. A general good agreement is found, with a correlation coefficient of 95%. Although this must be consolidated by including more eruptions in the analysis, these results already constitute a valuable element of validation.

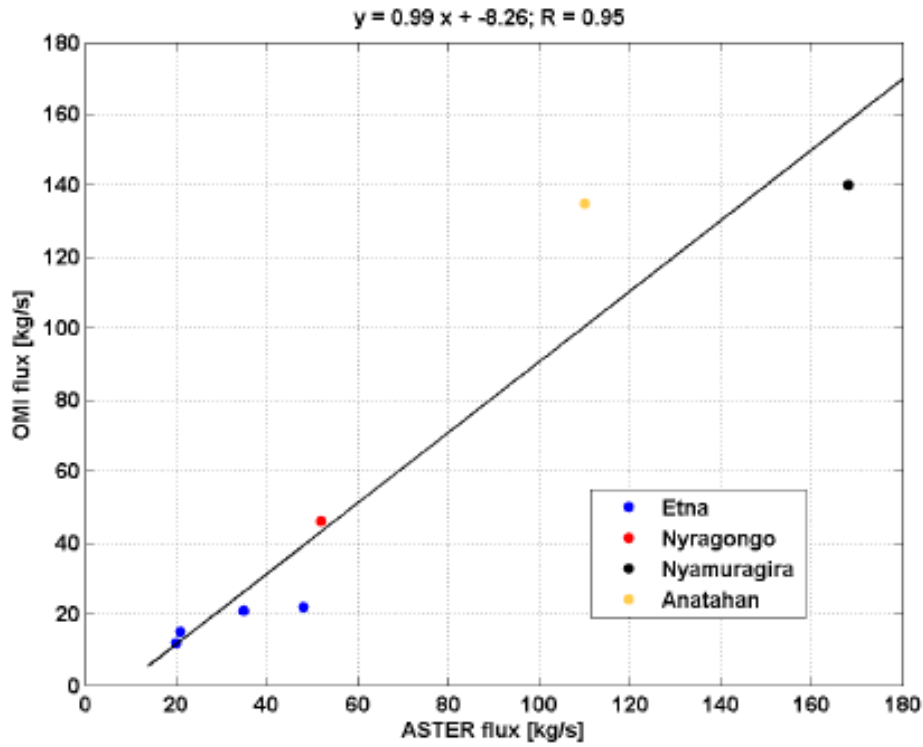



Figure 11: Correlation plot of the fluxes obtained from ASTER and OMI data over Etna (03/08/2006, 12/08/2006, 16/09/2007, 21/06/2008), Nyriagongo (18/01/2010), Nyamuragira (19/06/2007) and Anatahan (14/06/2005). Courtesy of R. Campion (ULB).

	<b>SACS+</b> Product Validation Document	<b>Ref.</b> SACSplus_PVD <b>Issue:</b> 1.0 <b>Date:</b> 10-12-2010 <b>Page:</b> 16 of 32
--	---	---

### 3 Comparison against ground-based measurements

This section describes a comparison of SO<sub>2</sub> total columns derived from measurements by GOME-2, SCIAMACHY and OMI against a few selected data sets of ground-based instruments, focussing on an SO<sub>2</sub> cloud originating from the Kasatochi volcanic eruption and passing over two ground stations in Europe. The ground-based data are based on direct-sun measurements from Brewer double-septrometers based at Uccle (Belgium) and Manchester (UK). The data are kindly provided by Hugues De Backer from the Belgium Royal Meteorological Institute (KMI-IRM) and John Rimmer of the University of Manchester (UK), respectively.

The SO<sub>2</sub> released into the atmosphere by the eruption of the Kasatochi volcano, was transported across the Northern Hemisphere by stratospheric winds in a few “branches” during August 2008. The path these branches followed after the initial emission depended on the altitude reached by the SO<sub>2</sub>. One of the branches passed over the ground stations in Uccle and Manchester on 17-18 August (see Figure 12), where groundstations with Brewer spectrometers measure ozone and SO<sub>2</sub> concentrations.

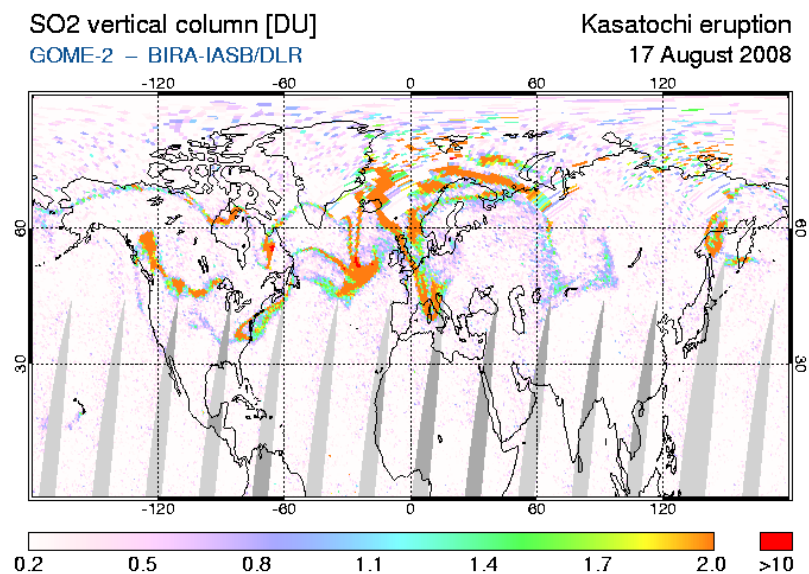



Figure 12: Distribution of SO<sub>2</sub> over the Northern Hemisphere on 17 August 2008, as seen by GOME-2.

Figures 13 and 14 show a comparison of the daily averaged ground-based data with satellite overpass data (50 km around the station). For the latter, the SO<sub>2</sub> data sets for the lower stratosphere were used. The Brewer data for Uccle showed an offset of +1.0 DU (the average over all data points from 1 to 15 August); this offset has been corrected for in the graphs. The Brewer data for Manchester showed no offset (the average over the data from 1 to 15 August is 0.02 DU).

The Brewer spectrometers are calibrated using reference instruments and this calibration is usually focussing on ozone. This means that SO<sub>2</sub> measurements and their calibration are secondary. For the calculation of the SO<sub>2</sub> concentration, a set of weighting coefficients is applied to the raw data when calculating the ratios used to derive the ozone concentration. These coefficients are designed to eliminate SO<sub>2</sub> and



	<b>SACS+</b> Product Validation Document	<b>Ref.</b> SACSplus_PVD <b>Issue:</b> 1.0 <b>Date:</b> 10-12-2010 <b>Page:</b> 17 of 32
---	---	---

aerosols from the ozone calculation. The sum  $\text{SO}_2 + \text{O}_3$  is then calculated using a different set of weighting coefficients, designed to optimise for  $\text{SO}_2$ . The previously calculated ozone is then subtracted to leave the  $\text{SO}_2$  concentration. These weighting coefficients are instrument specific, but in fact they are assumed to be the same for all Brewers and hard wired into the software, which means that the first calculation of  $\text{O}_3$  is affected by some fraction of the  $\text{SO}_2$  and aerosols. In the case of Manchester, for example, this leads to an underestimation of the  $\text{O}_3$  by up to about 40% of the  $\text{SO}_2$  present in the optical path. This means that subtracting the  $\text{O}_3$  from the  $\text{SO}_2 + \text{O}_3$  measurement may lead to an overestimated  $\text{SO}_2$  value. (John Rimmer, Manchester Univ.; priv.comm.)

Comparing the daily averaged data gives very good results in these two cases (Figures 13 and 14). Both the satellite and the Brewer measurements capture the enhanced  $\text{SO}_2$  columns over Uccle and Manchester very well. The comparison uses daily averages of the Brewer data because it is often difficult to compare individual measurements: ground-based measurements are rarely at exactly the same moment as satellite observations. And, more importantly, satellite instruments – with their large foot print – observe a different air mass than the ground-based instruments, since the latter perform point measurements.

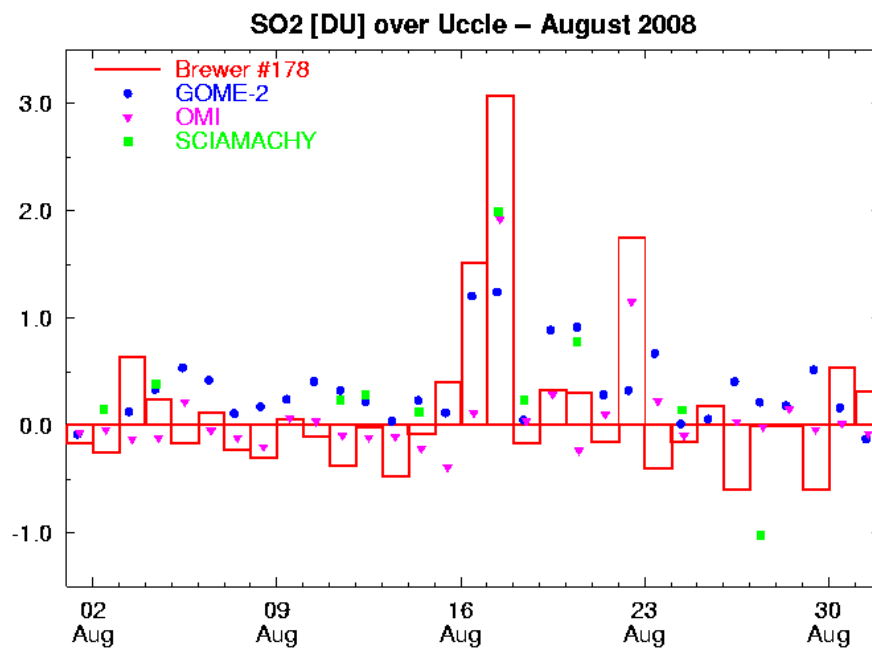


Figure 13: Comparison of  $\text{SO}_2$  total column data [in DU] as measured by the double Brewer of the Belgian Royal Meteorological Institute (KMI-IRM) in Uccle during August 2008 with satellite overpass data. The data is displayed in UTC time.

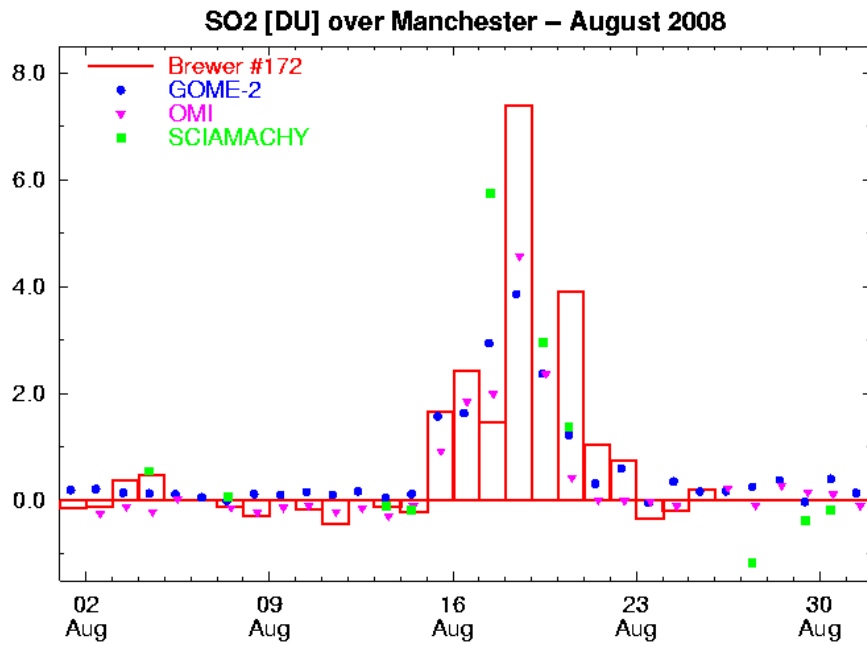



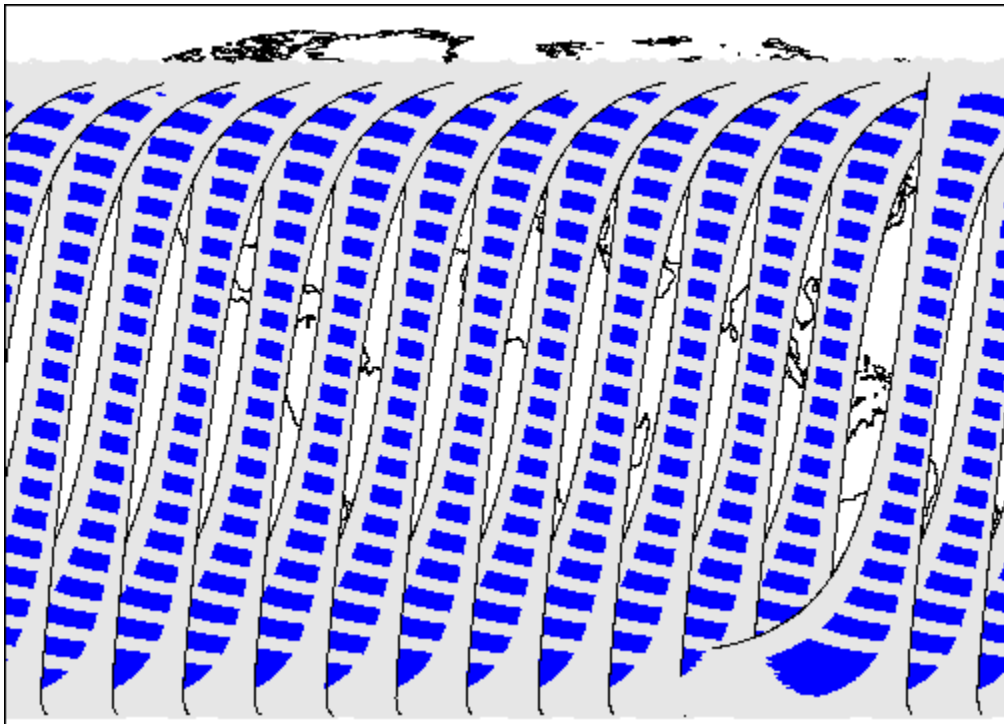
Figure 14: Comparison of SO<sub>2</sub> total column data [in DU] as measured by the double Brewer of the University of Manchester (UK) during August 2008 with satellite overpass data. Due to technical problems with the Brewer, the ground-based measurements end on 25 August. The data is displayed in UTC time.

	<b>SACS+</b> Product Validation Document	<b>Ref.</b> SACSplus_PVD <b>Issue:</b> 1.0 <b>Date:</b> 10-12-2010 <b>Page:</b> 19 of 32
---	---	---

## 4 Intercomparison of AAI satellite data products

### 4.1 Short Introduction


This chapter is based on the intercomparison study between GOME-2 and SCIAMACHY AAI data performed within the O3MSAF project. In this chapter we perform a direct comparison between (i) the AAI measured by GOME-2, and (ii) the AAI measured by SCIAMACHY (at roughly the same time and place). Because of the slightly different orbital periods, such an intercomparison is not possible for all days of the year. However, this is not a problem, as will be explained further on. For the many days on which intercomparison is possible, the orbit tracks overlap completely, ensuring that the scattering geometries (i.e., viewing and solar angles) are nearly identical, which adds to credibility and reliability of the intercomparison.



*Figure 15: Graphical explanation of the approach that was followed to compare the GOME-2 AAI's with those determined by SCIAMACHY. The black curves indicate the borders of the GOME-2 swaths. The blue boxes indicate the individual SCIAMACHY footprints. The data are from 17 October 2007.*

### 4.2 Intercomparison approach

Figure 15 explains the approach that was followed in a graphical way. For a given day, in this case 17 October 2007, we gather all SCIAMACHY and GOME-2 AAI orbits that are available to us. For each SCIAMACHY orbit, we determine, in an intelligent way,


	<b>SACS+</b> Product Validation Document	<b>Ref.</b> SACSplus_PVD <b>Issue:</b> 1.0 <b>Date:</b> 10-12-2010 <b>Page:</b> 20 of 32
---	---	---

the equator passing point (EPP). Using this information, we look for the GOME-2 orbit that has a more or less identical EPP. If this orbit exists, then we have a match. Note that, because of the different equator passing times (GOME-2: 09:30 LT; SCIAMACHY: 10:00 LT), there is a 30-minutes time difference. Related to this, there is also a slight difference in the solar zenith angle (SZA) which goes up to 7 degrees near the equator.

After that, we concentrate on all SCIAMACHY forward scan pixels between 70° N and 70° S that have a solar zenith angle below 80°. For all the pixels in this subset, we start looking for the GOME-2 forward scan pixels that belong to it, record their residues, and take the mean if more than one are found. The result we will call the “collocated GOME-2 AAI” from now on. We can then analyse the results, as shown in Fig. 16. Here we plotted the collocated GOME-2 AAI versus the original SCIAMACHY AAI. The agreement is rather good, although there is quite some scatter around the expected one-to-one relationship. This scatter can be explained by a number of reasons.

First of all, we have a 30-minutes time difference between SCIAMACHY and GOME-2, which could lead to a change in the observed scene in the case of clouds. By filtering out cloudy scenes we could indeed reduce the scatter a bit, of course at the expense of the number of available data points. Secondly, there is a difference in the solar zenith and azimuth angles of SCIAMACHY and GOME-2. Thirdly, and most importantly, the SCIAMACHY and GOME-2 footprints do not overlap completely, so there will always be a spatial collocation mismatch between the SCIAMACHY and GOME-2 footprints. We took no action to improve on this, because the goal here is to analyse the entire collection of data as a whole, not to improve the intercomparison of individual ground pixels.

In Fig. 16 we also present a red line, which is a linear fit to the data points. Weighted fitting was not applied, but residues with values lower than -10 and higher than +10 were not trusted and were therefore not allowed to take part in the fitting process. For the specific day shown in Fig. 15, 13 July 2008, the slope was found to be  $1.01 \pm 0.03$  and the intercept was  $0.95 \pm 0.05$ , pointing to an offset of the GOME-2 AAI w.r.t. the SCIAMACHY AAI. Note that the SCIAMACHY AAI was found to be well calibrated w.r.t. GOME-2's predecessor GOME-1 (see, for instance, *Tilstra et al.* [2007]).

	<b>SACS+</b> Product Validation Document	<b>Ref.</b> SACSplus_PVD <b>Issue:</b> 1.0 <b>Date:</b> 10-12-2010 <b>Page:</b> 21 of 32
---	---	---

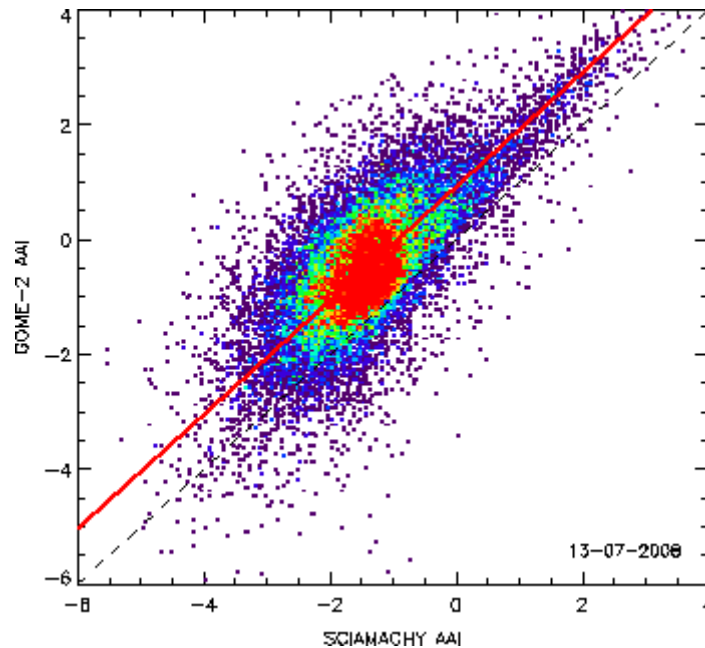



Figure 16: The “collocated GOME-2 AAI” versus the SCIAMACHY AAI, for 13 July 2008. The agreement is fair, considering the fact that we took no effort to improve handling the spatial mismatch between the SCIAMACHY and GOME-2 footprints. The red line is a linear fit to the data points.

### 4.3 First results – time series A

The analysis described in the previous section was performed on the entire GOME-2 AAI reprocessed data set that was available. This data set covers most of the years 2007 and 2008. While processing the data set, we recorded the number of orbits for which we could successfully link the SCIAMACHY data to GOME-2 data. When a SCIAMACHY monitoring orbit was encountered (narrow swath, nadir static, et cetera), then this orbit was skipped altogether. When a GOME-2 narrow swath or nadir static orbit was encountered, this orbit was not skipped, but it was recorded that a narrow swath/nadir static orbit was used that day. We decided to remove days with more than two of such orbits from the analysis.

Because of the slightly different orbital periods of SCIAMACHY and GOME-2, in general the orbit tracks of the two instruments do not overlap. Every nine days, however, the situation occurs that they do overlap, for a relatively short period of  $\sim 2$  days (depending on how strict we are). For each day for which we could find SCIAMACHY and GOME-2 orbits with overlapping orbit tracks, we recorded the number of these orbits. Slope and intercept of the linear fit to the collocated AAI's, performed in the way described before, were also recorded. In Fig. 17, we plotted the resulting slopes as a function of time. The red circles are results which in our opinion are not reliable, either because there were not enough orbit track overlaps found (say, less than 10), or because there were two or more narrow swath/nadir static orbits involved. The blue circles are the remaining results, which we expect to be reliable.

	<b>SACS+</b> Product Validation Document	<b>Ref.</b> SACSplus_PVD <b>Issue:</b> 1.0 <b>Date:</b> 10-12-2010 <b>Page:</b> 22 of 32
--	---	---

As can be seen, the red circles are scattered, but the blue circles are rather consistent in their behaviour. At first sight, there appears to be a good correlation between the SCIAMACHY and GOME-2 residues, with a slope very close to one. On the other hand, there seems to be a periodic or seasonal variation hidden behind the scatter in the slopes. In Fig. 17, we plotted the intercepts of the linear fits. It is clear from this plot that there is an offset in the residue of GOME-2 w.r.t. SCIAMACHY. The nature of this offset must be a discrepancy in the radiometric calibration of GOME-2. Note that the offset is not dramatic. A one index point offset can already be explained by a 2% error in the reflectance (*de Graaf et al. [2005]*).

As for the time dependence of the slopes and intercepts shown in Figs. 17 and 18, we have to conclude that – at least within the accuracy of the intercomparison – no clear systematic time dependence was found. This is expected for the slopes, because radiometric calibration errors only slightly affect the slopes, while strongly affecting the intercepts. The intercepts also show no clear time dependence, with only a slight tendency to lower values at the end of the time series. This would indicate that the GOME-2 residue has been reasonable stable over the last two years covered by the time series.

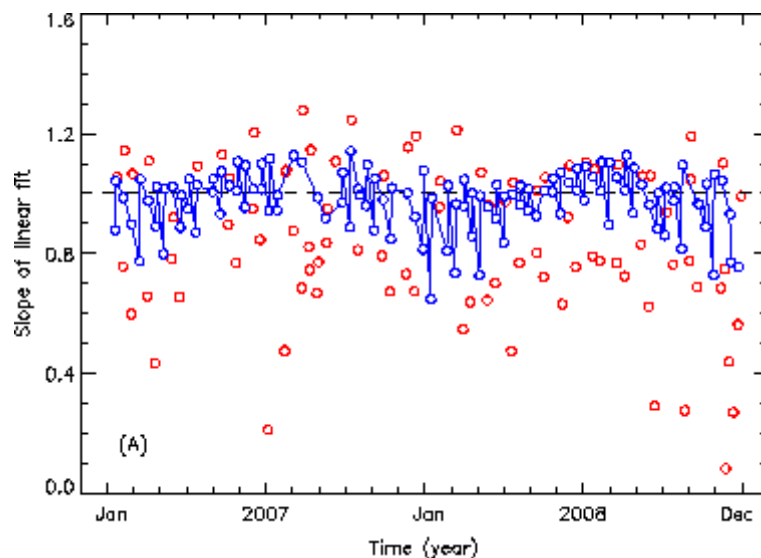



Figure 17: Slope of the linear fits to the (GOME-2 versus SCIAMACHY) data points as a function of time. The red circles are unreliable: not enough orbits with perfect orbit track overlap between SCIAMACHY and GOME-2, and/or too many GOME-2 narrow swath orbits included. The blue circles are believed to be reliable, although some scatter is obviously present in the blue data points.

	<b>SACS+</b> Product Validation Document	<b>Ref.</b> SACSpplus_PVD <b>Issue:</b> 1.0 <b>Date:</b> 10-12-2010 <b>Page:</b> 23 of 32
--	---	--

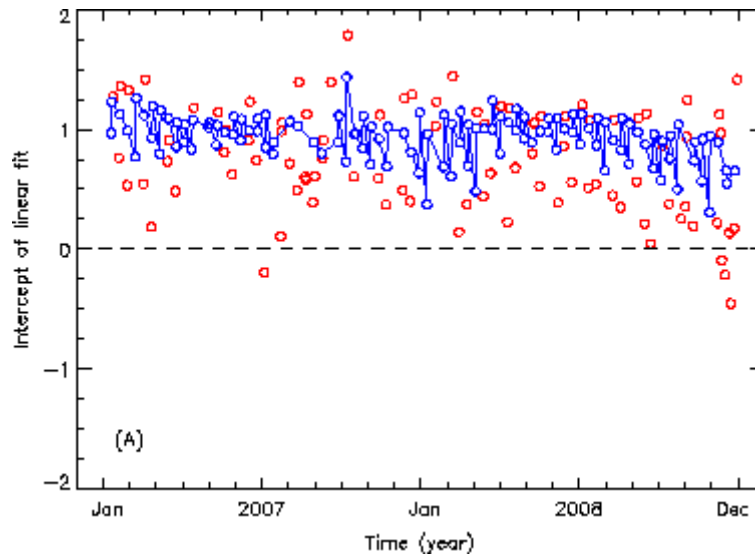


Figure 18: Intercept of the linear fit. The colour coding and its meaning are the same as in Fig. 17. The result shows that there is a clear offset of GOME-2 w.r.t. SCIAMACHY, of roughly one index point.

#### 4.4 Improving the intercomparison – time series B

The statistical errors on slope and intercept, determined in the linear fitting process as illustrated in Fig. 16, are both on the order of 0.05. This is much less than the large variability that is actually found in Figs. 17 and 18. The much larger error is caused by a systematic error, namely the unavoidable misalignment between the SCIAMACHY and GOME-2 orbits. Figure 15 explains this more clearly. For the day in question, 17 October 2007, the first SCIAMACHY and GOME-2 orbits have near perfect overlap, but at the end of the day, the overlap is already quite poor. For the previous day, i.e., 16 October 2007, the situation is exactly the other way around. The best thing to do in this particular case would be to take the last ~7 orbits of 16 October 2007, and the first ~7 orbits of 17 October 2007, and to glue these together to form an artificial “new day”. The resulting collection of orbits of this “new day” would have a much better average alignment than the collection of orbits of the two original days.

We therefore abandon the idea of letting each day start at 00:00 UTC and instead determine a careful selection of subsequent orbits for which the misalignment, in the absolute sense, is below a certain threshold. The threshold used was 1.6 degrees (in longitudes) which in normal situations yields between 14 and 17 orbits that fulfill this criterion. The artificial days created this way cover a time period of 24 hours, i.e., are spread out over the entire longitude range of the globe. Figure 19 shows the relative longitudinal alignment for a selection of associated SCIAMACHY and GOME-2 orbits taken from 26 and 27 February 2007. All selected orbits have an absolute relative longitudinal alignment less than 1.6 degrees.

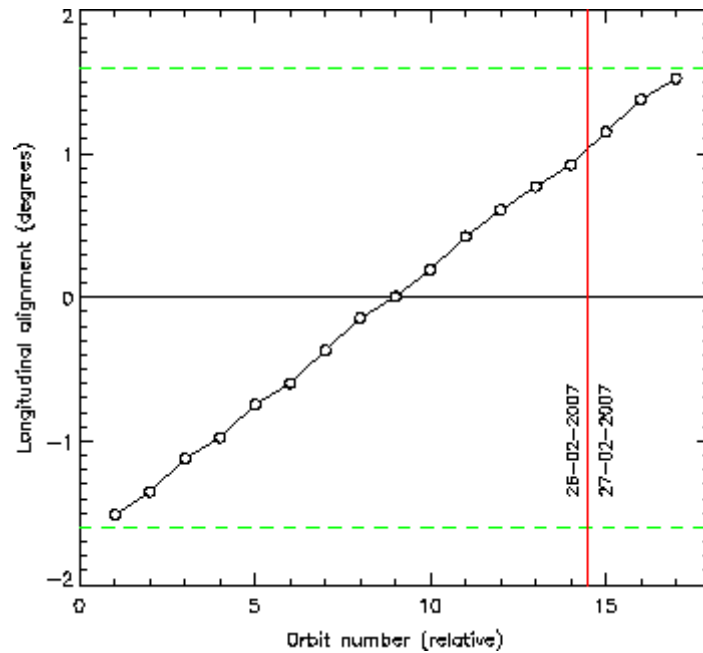


Figure 19: Longitudinal alignment for a selection of associated SCIAMACHY and GOME-2 orbits taken from 26 and 27 February 2007. All orbits have a longitudinal misalignment less than 1.6 degrees.

In Fig. 20 we present again a time series of the slope of the linear fit to the data points in the scatterplots, but now for the artificial “new days” we created. As before, the red circles indicate days for which not enough orbits were available. Narrow swath and nadir static orbits were not considered. Also compare with Fig. 17. Clearly, the variability in the slopes has been reduced enormously. It now amounts to roughly 0.01–0.03, which relates well to the statistical errors reported from the fitting processes. This confirms that we have removed an important error source from the intercomparison approach.

The improved accuracy, and the resulting reduced variability, now reveal that there is a seasonal variation found in the SCIAMACHY versus GOME-2 intercomparison, at least for the slope of the linear fit. The existence of a seasonal variation in the slope is not understood, and will be examined more closely in the next section. In Fig. 21 we present a time series of the intercept of the linear fit to the data points in the scatter plots, for the artificial “new days”. The variability has been reduced, and now we can discern a very mild seasonal variation on top of a small downwards trend.

Figure 22 presents the standard deviation  $\sigma$  of the GOME-2 versus SCIAMACHY data points in relation to the achieved linear fit. That is, if the GOME-2 AAI’s are represented by the array  $y_i$ , and the SCIAMACHY AAI’s are represented by the array  $x_i$ , and the best linear fit to the data can be represented by  $y = mx+n$ , where  $m$  is the slope and  $n$  is the intercept of the linear fit, then the standard deviation is defined as  $\sigma(y_i - mx_i - n)$ . The standard deviation is on the order of 0.5 index points. Note that this means that the (bias-corrected) GOME-2 AAI is therefore shown to be validated against the SCIAMACHY AAI within an accuracy  $\sim 0.5$  index points. Also note that, although we went through a great deal of trouble to achieve an as accurate as possible intercomparison, there is still an inaccuracy to be attributed to the intercomparison



procedure itself. That is, the “real” uncertainty in the GOME-2 AAI will be less than standard deviation of  $\sim 0.5$  index points reported here, because the standard deviation also includes inaccuracies introduced by the intercomparison approach (and its intrinsic imperfections).

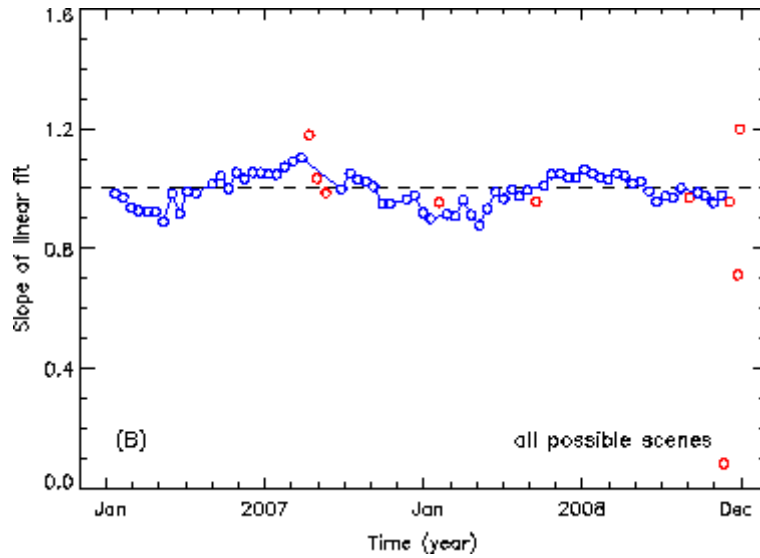


Figure 20: Slope of the linear fits to the (GOME-2 versus SCLAMACHY) data points as a function of time, for the new approach in which artificial days are created (approach B, see text). The red circles are believed to be unreliable: not enough orbits and/or too many GOME-2 narrow swath orbits included.

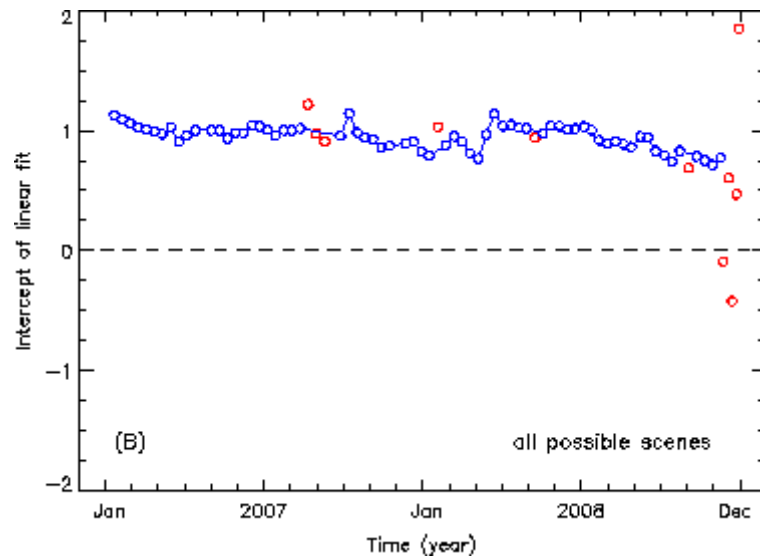



Figure 21: Intercept of the linear fit, for the new approach B in which artificial days are created. The colour coding and meaning is the same as in Fig. 20. The result shows that there is a clear offset of GOME-2 w.r.t. SCLAMACHY, of roughly one index point. The red circles are believed to be unreliable.

	<b>SACS+</b> Product Validation Document	<b>Ref.</b> SACPlus_PVD <b>Issue:</b> 1.0 <b>Date:</b> 10-12-2010 <b>Page:</b> 26 of 32
---	---	--

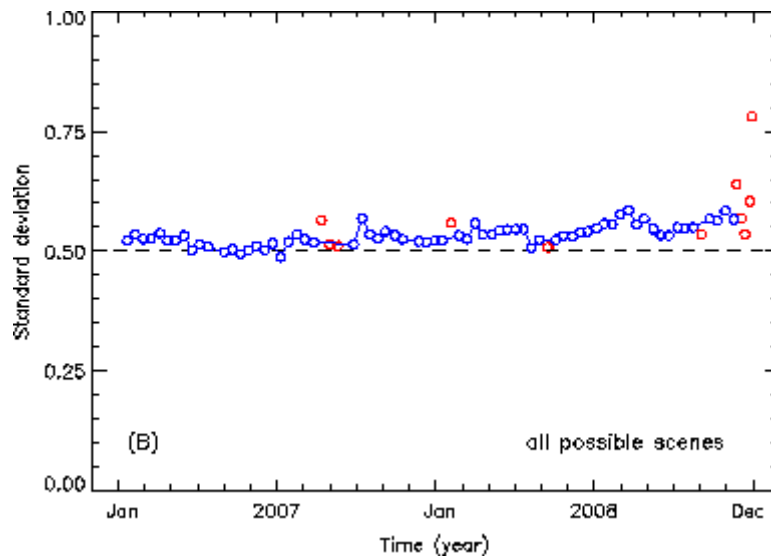


Figure 22: Standard deviation of the difference between linear fit and the data, for the new approach B in which artificial days are created. The standard deviation is roughly 0.5 index points, showing a slight increase with time. As before, the results for the red circles were believed to be unreliable beforehand.


## 4.5 Scene dependencies

In this subsection we will perform a re-analysis of the results, this time discriminating between different scene types. This is necessary, because the results of the previous section showed indications of a small seasonal variation. The presented slopes oscillated mildly around the expected one-to-one relationship. We have to exclude the possibility that the low aerosols loads in the months October to December, resulting in an absence of data with positive residues, affect the linear fit a negative way, thereby possibly creating a seasonal dependence in the time series. We discriminate between the following scene types:

1. cloudy scenes: SCIAMACHY FRESCO+ cloud fraction  $\geq 0.1$
2. clear sky scenes: SCIAMACHY FRESCO+ cloud fraction  $< 0.1$  and SCIAMACHY residue  $< 0.5$
3. aerosol loaded scenes: SCIAMACHY residue  $\geq 0$

The resulting time series of slope and intercept of the linear fits to the GOME-2 versus SCIAMACHY data points are shown in Figs. 23–28. Both the slope and intercept found for the subset of cloudy scenes turns out to be similar to the overall case shown in Figs. 20 and 21, where all scenes were taken into account. This is perfectly understandable, as most of the observations are in fact cloud contaminated, and cloudy scenes therefore determine the overall case.

The slopes found for the clear sky case show no clear seasonal variation, and are equal to one. Note that the retrieved intercepts are about 0.3 index points lower than the intercepts found for the cloudy case. The slopes of the aerosol loaded cases show a large scatter, due to the low number of aerosol loaded scenes and the small residue range on which to perform the fit. A seasonal variation might or might not be present, it is

	<b>SACS+</b> Product Validation Document	<b>Ref.</b> SACPlus_PVD <b>Issue:</b> 1.0 <b>Date:</b> 10-12-2010 <b>Page:</b> 27 of 32
--	---	--

impossible to judge from the results presented in Fig. 27. The time series of the intercept shows less scatter, but the intercepts are on average 0.5 index points lower than the intercepts of overall case. Also, it is the only subset which does not show a downward trend in the intercepts.

To be able to study the behaviour of the aerosol loaded scenes we gather all SCIAMACHY and GOME-2 AAI measurements of the year 2007 and 2008 found using the approach described in Sect. 4.4 (method B). The biases found in Fig. 21 were subtracted from the GOME-2 AAI measurements, so the GOME-2 AAI's are bias-corrected. Figure 29 presents the GOME-2 versus SCIAMACHY scatter plot of these data. The blue curve is a linear fit to the data, with slope  $1.01 \pm 0.01$ . The red curve is a fit to the subset of measurements of aerosol loaded scenes. The slope is  $0.97 \pm 0.03$ , very close to one. This proves that, averaged over two years, there is indeed a near one-to-one relationship found between the SCIAMACHY and GOME-2 AAI for aerosol loaded scenes.

In conclusion, we found an indication of a small seasonal variation in the GOME-2 versus SCIAMACHY intercomparison results. It is possible that the seasonal variation is real, but it could also be artificial, i.e., an artefact of the intercomparison itself. Possibly the seasonal variation is caused by the seasonal variation in global aerosol loads, which in turn could affect the fitting results. The results of this section, however, do not provide a clear proof for this. At the same time, the intercomparison might also be affected by the fact that the SCIAMACHY and GOME-2 measurements have a slightly different solar zenith angle. This could lead to a seasonal variation having the right period and phase.

If the seasonal variation is real, then it is most likely a radiometric calibration problem. The algorithm of the SCIAMACHY AAI is very similar to the algorithm of the GOME-2 AAI. Note that we cannot fully exclude the possibility that SCIAMACHY causes the seasonal variation, although we should also point out that this instrument has been found to be well-calibrated w.r.t. GOME-1.

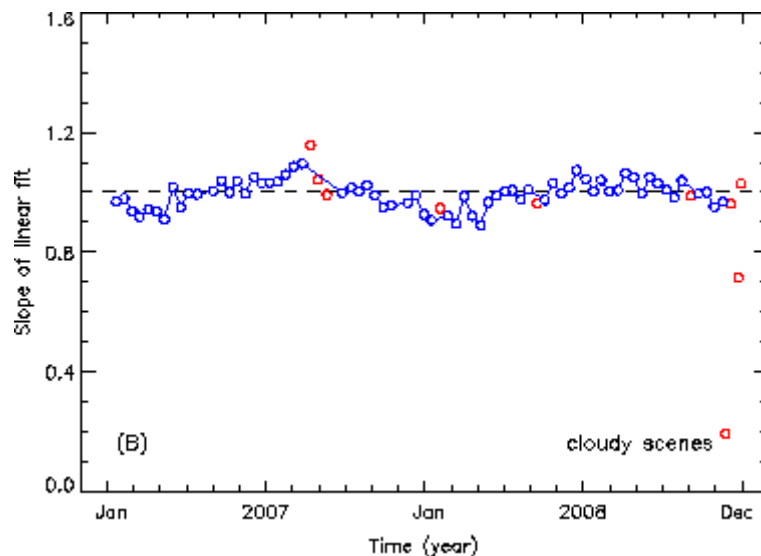


Figure 23: Slope of the linear fit for cloudy scenes, according to the validation method described in Sect. 4.4 The SCIAMACHY FRESCO+ cloud fraction was larger than 0.1 for all measurements.

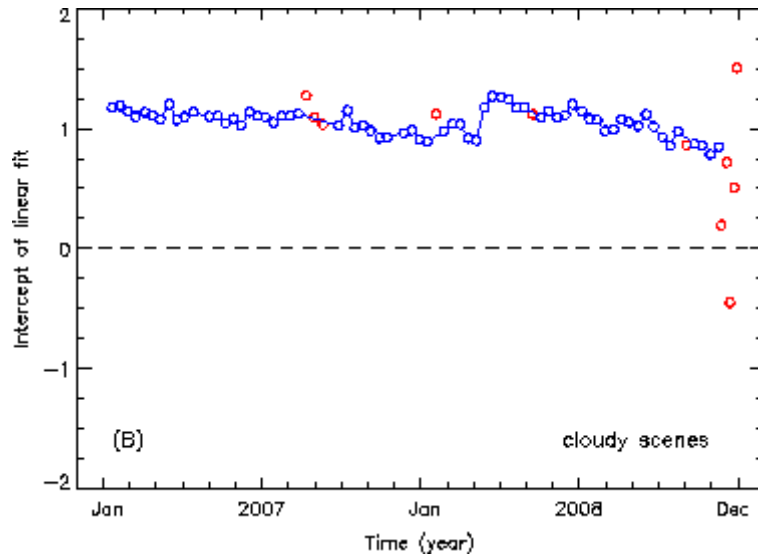


Figure 24: Intercept of the linear fit for cloudy scenes, according to the validation method described in Sect. 4.4. The SCIAMACHY FRESCO+ cloud fraction was larger than 0.1 for all measurements.

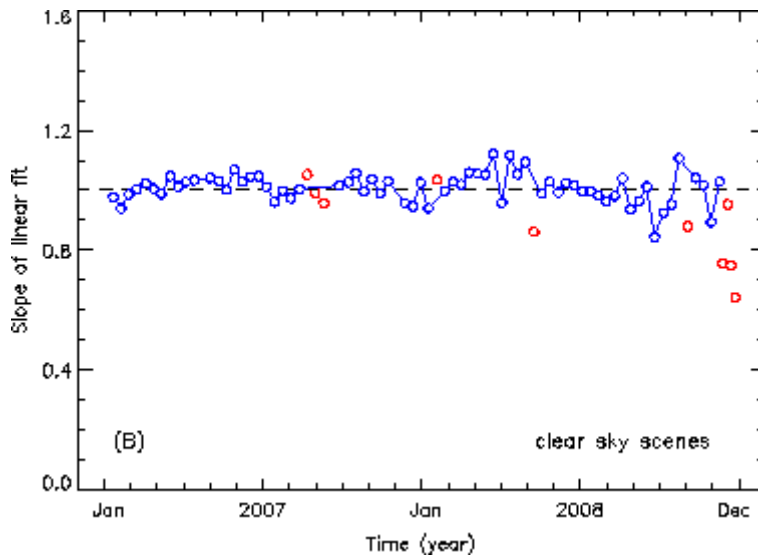



Figure 25: Slope of the linear fit for clear sky scenes, according to the validation method described in Sect. 4.4. FRESCO+ cloud fraction smaller than 0.1 and SCIAMACHY AAI smaller than 0.5.

	<b>SACS+</b> Product Validation Document	<b>Ref.</b> SACSplus_PVD <b>Issue:</b> 1.0 <b>Date:</b> 10-12-2010 <b>Page:</b> 29 of 32
---	---	---

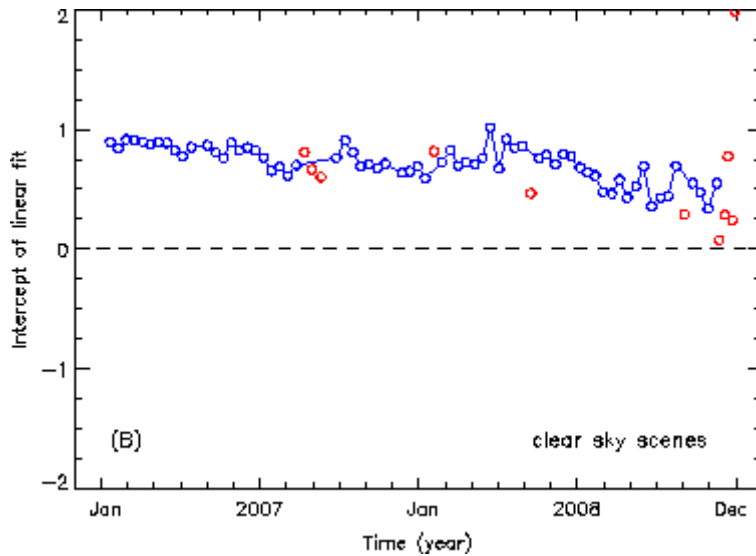


Figure 26: Intercept of the linear fit for clear sky scenes, according to the validation method described in Sect. 4.4. FRESCO+ cloud fraction smaller than 0.1 and SCIAMACHY AAI smaller than 0.5.

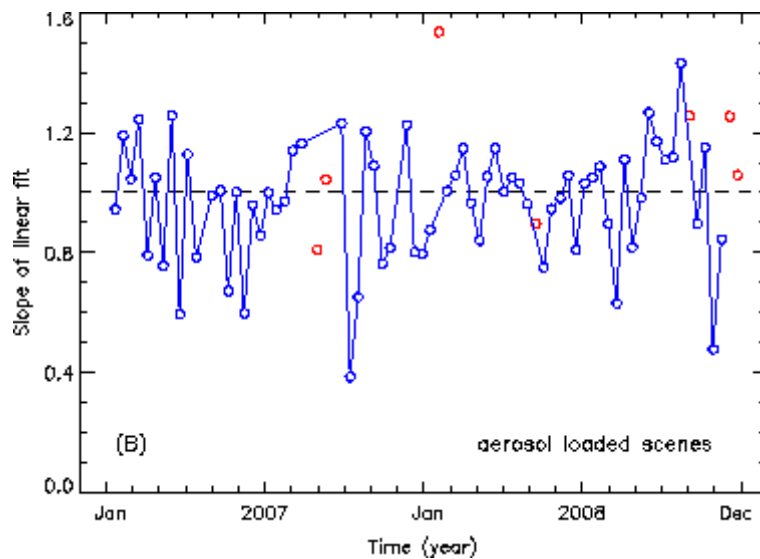



Figure 27: Slope of the linear fit for scenes with a sizeable aerosol load. The SCIAMACHY AAI was larger than 0.5 for all measurements. The large scatter in the data points is caused by the small number of data points having a positive residue. This is especially the case outside the aerosol season.

	<b>SACS+</b> Product Validation Document	<b>Ref.</b> SACSplus_PVD <b>Issue:</b> 1.0 <b>Date:</b> 10-12-2010 <b>Page:</b> 30 of 32
---	---	---

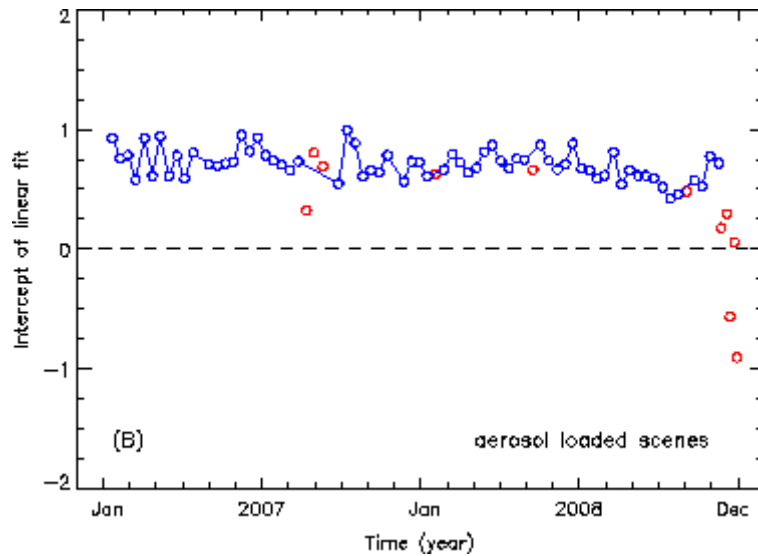


Figure 28: Intercept of the linear fit for scenes with a sizeable aerosol load. The SCIAMACHY AAI was larger than 0.5 for all measurements used.

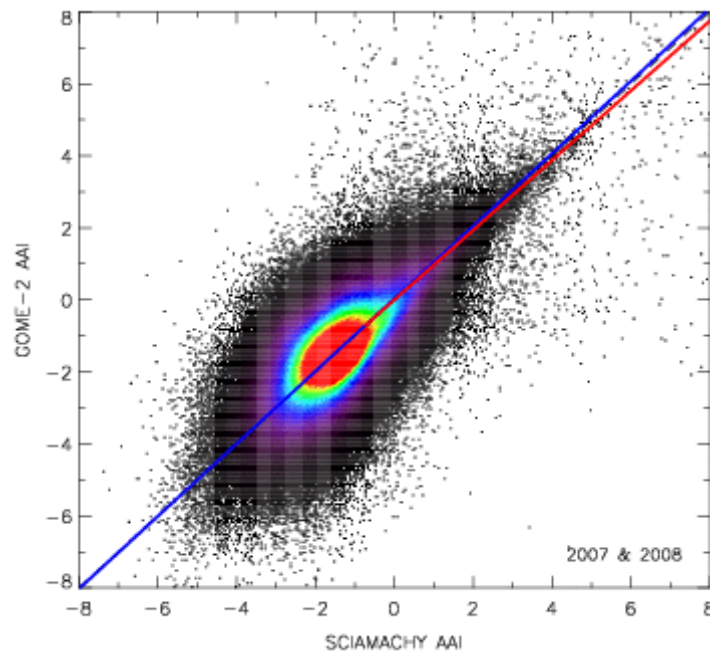



Figure 29: The collocated GOME-2 AAI versus the SCIAMACHY AAI, taken from all the 81 artificial days found in 2007 and 2008 for which the collocation is nearly perfect. The GOME-2 AAI's were biascorrected. The blue curve is a linear fit to the data, with slope  $1.01 \pm 0.01$ . The red curve is a fit to the subset of measurements of aerosol loaded scenes. The slope is  $0.97 \pm 0.03$ .

## 4.6 Discussion of results


The results seem to indicate that there is a good correlation between the GOME-2 AAI and the SCIAMACHY AAI, which was used as a reference. The correlation is good in the sense that (i) there is a clear linear relationship between the GOME-2 AAI and the

	<b>SACS+</b> Product Validation Document	<b>Ref.</b> SACSpus_PVD <b>Issue:</b> 1.0 <b>Date:</b> 10-12-2010 <b>Page:</b> 31 of 32
---	---	--

SCIAMACHY AAI, and (ii) the slope of the linear fit to the GOME-2 versus SCIAMACHY data points is close to one. On the other hand, there is an offset present in the GOME-2 AAI. This offset is most likely related to errors in the radiometric calibration.

The bias-corrected uncertainty in the GOME-2 AAI was found to be ~0.5 index point. As explained in Sect. 4.4, this is only an upper limit, because this value is also determined by the quality of the SCIAMACHY AAI and the quality of our intercomparison approach. Using the validation technique described in this chapter, it is not possible to reach a higher accuracy for the intercomparison results.

Please note that by using SCIAMACHY as a reference, the results in principle only apply to residues coming from the inner part of the GOME-2 swath, i.e., observations for which the viewing zenith angle (VZA) is below ~33°. It is also important to mention again that we made use of forward pixels only. Backscan pixels were not taken into account in the analysis, and the results therefore only apply to the GOME-2 measurements that were performed in the forward scan of the instrument.

	<b>SACS+</b> Product Validation Document	<b>Ref.</b> SACSplus_PVD <b>Issue:</b> 1.0 <b>Date:</b> 10-12-2010 <b>Page:</b> 32 of 32
---	---	---

## 5 References

Campion, R.A., Salerno, G.G., Coheur, P.-F., Hurtmans, D., Clarisse, L., Kazahaya, K., Burton, M.R., Caltabiano, T., Clerbaux, C., Bernard, A.: Measuring volcanic degassing of SO<sub>2</sub> in the lower troposphere with ASTER band ratios, *Journal of Volcanology and Geothermal Research*, 194, Issues 1-3, pp 42-54, 2010.

de Graaf, M., P. Stammes, O. Torres, and R. Koelemeijer, Absorbing Aerosol Index: Sensitivity analysis, application to GOME and comparison with TOMS, *Journal of Geophysical Research*, 110, doi:10.1029/2004JD005,178, 2005.

Pieri, D., Abrams, M.: ASTER watches the world's volcanoes: a new paradigm for volcanological observations from orbit, *J. Volcano. Geotherm. Res.*, 135, 13-28, 2010.

Pinardi, G., Campion, R., Van Roozendaal, M., Fayt, C., Van Geffen, J., Galle, B., Carn, S., Valks, P., Rix, M., Hildago, S., Bourquin, J., Garzon, G., Inguaggiato, S., Vita, F.: Comparison of volcanic SO<sub>2</sub> flux measurements from satellite and from the NOVAC network, in *Proceedings of the EUMETSAT Meteorological Satellite Conference*, 20-24 September 2010, Cordoba, Spain, 2010.

Tilstra, L., M. de Graaf, I. Aben, and P. Stammes, Analysis of 5 years SCIAMACHY Absorbing Aerosol Index data, in *Proceedings of the 2007 Envisat Symposium*, ESA Special Publication SP-636, European Space Agency, ESA/ESTEC, Noordwijk, The Netherlands, 2007.

Van Geffen, J., Van Roozendaal, M., Rix, M., Valks, P.: Initial validation of GOME-2 GDP 4.2 SO<sub>2</sub> total columns – ORR B, EUMETSAT O3M SAF validation report, TN-IASB-GOME2-O3MSAF- SO2-01.1, 2008.